Acta Biomaterialia 7 (2011) 258–267

Contents lists available at ScienceDirect

Acta Biomaterialia

journal homepage: www.elsevier.com/locate/actabiomat

Synthesis, characterization and in vitro cell compatibility study of a poly(amic acid) graft/cross-linked poly(vinyl alcohol) hydrogel

Donna T. Padavan [a,b], Amanda M. Hamilton [c,d], Leonardo E. Millon [b,e], Derek R. Boughner [a,c,d], Wankei Wan [a,b,d,*]

[a] Biomedical Engineering Graduate Program, The University of Western Ontario, London, Ontario, Canada N6A 5B9
[b] Fordham Center for Biomedical Engineering, Department of Chemical and Biochemical Engineering, The University of Western Ontario, London, Ontario, Canada N6A 5B9
[c] Department of Anatomy and Cell Biology, The University of Western Ontario, London, Ontario, Canada N6A 5B9
[d] Robarts Research Institute, The University of Western Ontario, London, Ontario, Canada N6A 5B9
[e] Axcelon Biopolymers Corporation, The University of Western Ontario, London, Ontario, Canada N6A 5B9

ARTICLE INFO

Article history:
Received 16 March 2010
Received in revised form 6 July 2010
Accepted 27 July 2010
Available online 3 August 2010

Keywords:
Poly(amic acid)
Poly(vinyl alcohol)
Esterification
Solid-state ^{13}C NMR
Mechanical testing

ABSTRACT

Although physically cross-linked poly(vinyl alcohol) (PVA) hydrogels have tunable mechanical properties to match that of soft tissues, such as vascular tissue, their hydrophilic nature is not conducive to cell adhesion and spreading. For applications such as small diameter vascular grafts for coronary bypass both mechanical matching and hemocompatibility are important. Poly(amic acid) (PAA), derived from ethylene diamine tetraacetic dianhydride, is a cell-compatible polymer. It was grafted/cross-linked onto physically cross-linked PVA to provide cell compatibility. Functionalization was achieved via a one-step esterification reaction using 1,3-dicyclohexylcarbodiimide as the coupling agent and 4-dimethylaminopyridine as the catalyst. The success of the grafting reaction was verified using Fourier transform infrared spectroscopy, solid-state nuclear magnetic resonance spectroscopy and X-ray photoelectron spectroscopy. The mechanical properties of the starting PVA hydrogel were largely preserved after the grafting reaction within the physiological strain range of vascular tissue. In vitro cell culture studies using primary porcine endothelial cells confirmed cell compatibility of the PAA graft PVA hydrogel, making it an attractive candidate for small diameter vascular graft development.

1. Introduction

Biocompatible hydrogels are promising materials that are attractive for a broad range of biomedical applications, ranging from medical devices to tissue regeneration scaffolds [1,2]. However, among these biocompatible hydrogels, not all are cell compatible. This is especially true of those with very high water contents. A prominent example of this is the cross-linked poly(vinyl alcohol) (PVA) hydrogel. Its hydrophilic nature makes it difficult to support cell adhesion, viability and growth. Many approaches have been reported over the years to improve the cell affinity of PVA. These include phosphorylating the PVA surface [3], functionalizing PVA with fibronectin [4], immobilizing the RGD motif onto the PVA surface [5], blending PVA with starch [6], chitosan [7–9], gelatin [10] or carboxymethyl chitin [11], forming PVA composites with porcine small intestinal submucosa [12] and depositing hydroxyapatite onto the PVA surface [13]. Most of these methods reported have been applied to PVA that has been chemically cross-linked using reagents such as glutaraldehyde prior to surface modification.

Physically cross-linked PVA hydrogels prepared by the low temperature thermal cycling method is an attractive alternative in potential cardiovascular applications, since its mechanical properties can be tuned to closely match to that of soft tissues, such as vascular tissue [14,15]. In vascular graft applications a mismatch in mechanical properties between the graft material and native tissue at the suturing junction is believed to play a major role in postoperative complications and ultimate failure [16,17]. Methods are available to passivate the biomaterial surface to enhance hemocompatibility. The most common methods investigated include treating the polymer with bioactive agents such as heparin, growth factors and other anticoagulant peptide sequences [18]. Another approach is to promote endothelialization of the surface by functionalizing it with an adhesive extracellular glycoprotein (fibronectin) or amino acid sequence (RGD). Millon et al. succeeded in functionalizing physically cross-linked PVA with fibronectin (results submitted for publication) using a reaction without the carbonyl diimidazole activation step normally required for chemically cross-linked PVA. However, drying and re-swelling of the PVA

* Corresponding author at: Fordham Center for Biomedical Engineering, Department of Chemical and Biochemical Engineering, The University of Western Ontario, London, Ontario, Canada N6A 5B9. Tel.: +1 519 661 2111; fax: +1 519 850 2308.
E-mail address: wkwan@eng.uwo.ca (W. Wan).

1742-7061/$ - see front matter © 2010 Acta Materialia Inc. Published by Elsevier Ltd. All rights reserved.
doi:10.1016/j.actbio.2010.07.038

hydrogel was still necessary. Cell compatibility was assessed by seeding endothelial cells (ECs) on the functionalized surface and observing cell adhesion, morphology and spreading for up to 24 h. The resulting PVA–fibronectin functionalized hydrogels had an elastic modulus that was about 56% higher than the original. This was a result of dehydrating and rehydrating the hydrogel, which was necessary for the functionalization reaction. In this case, one option to match the mechanical properties of aorta within the physiological strain range is to start with a softer PVA hydrogel (lower thermal cycling). To preserve the original mechanical properties of PVA an alternative is to use a functionalizing approach that does not require a dehydration–rehydration step.

Recently, Padavan et al. [19] synthesized a poly(amic acid) (PAA) polymer based on ethylene diamine tetraacetic dianhydride containing amide and carboxylic acid functional groups. In in vitro cell compatibility assessments of this material vascular cells (radial artery cells and ECs) adhered to, spread and proliferated at comparable rates to that of the controls.

In this paper, we report a new strategy for cell compatibility of physically cross-linked, mechanically tuned PVA hydrogels by grafting/cross-linking the cell-compatible PAA onto a PVA hydrogel (PAA-g/c-PVA) via an esterification pathway that does not require dehydration of the hydrogel. Surface functionalization of PVA is achieved using a one-step esterification reaction, free of protecting groups, as opposed to a multi-step reaction. Primary porcine aortic ECs were used for cell compatibility studies, as they are relevant to cardiovascular tissue replacement applications.

2. Materials and methods

2.1. Materials

PVA (molecular weight 146–186 $\times 10^3$, hydrolysis 99%), high purity (98%) ethylene diamine tetraacetic dianhydride (EDTAD), 4-dimethylaminopyridine (DMAP), 1,3-dicyclohexyl carbodiimide (DCC) and the polymerization reaction solvents N-methyl-2-pyrrolidone (NMP) and N,N-dimethylformamide (DMF) were purchased from Sigma–Aldrich. The solvents were dried over molecular sieves having a nominal pore diameter of 3 Å and filtered prior to use. Paraphenylene diamine (PPD) was purchased from Thermo Fisher Scientific Co. (Acros, Belgium) and used as received. All other chemicals were purchased from VWR and Sigma–Aldrich.

2.2. PVA, PAA and PAA-g/c-PVA polymer synthesis

2.2.1. Preparation of PVA hydrogel

The preparation of physically cross-linked PVA hydrogels has been previously described [14,20]. Briefly, a 10 wt.% PVA solution was prepared by heating (90 °C) and mixing (mechanical stirrer) the solution for 3 h. The PVA solution was then transferred to a custom made aluminum mold with a thickness of 150 μm and placed in a heated/refrigerated bath. The PVA solution was cycled six times between 20 °C and −20 °C to obtain cycle 6 samples, which were previously reported by Millon et al. as having excellent mechanical properties similar to those of cardiovascular tissue [14]. With each successive cycle physical cross-linking increased, forming polymer-rich and polymer-poor regions. Polymer-rich regions consisted of an amorphous phase (weak mesh of polymer chains) and crystallites, whereas polymer-poor regions consisted of porous structure due to melted ice crystals [21]. PVA samples were punched into smooth, circular discs having a diameter of 11 mm. Samples were placed in distilled water and stored at room temperature prior to grafting experiments.

For mechanical testing and scanning electron microscopy (SEM), the PVA samples were prepared using a mold with a 1.5 mm thick gasket prior to thermal cycling. Samples were cut into squares of 25 × 25 × 5 mm for tensile testing ($n = 5$) and immersed in phosphate-buffered saline (PBS) for 48 h prior to testing [14]. After mechanical testing these samples were critical point dried for SEM.

2.2.2. Preparation of poly(amic acid) solution

A PAA polymer solution was prepared via a condensation polymerization reaction as previously described [19]. Briefly, a 1 mol equivalent of PPD was placed into a 100 ml, three necked, round bottomed flask and dissolved in DMF or NMP at 37 °C. A 1 mol equivalent of EDTAD was then added to the PPD solution and the chosen reaction solvent. Nitrogen gas (N_2) was purged continuously throughout the experiment. The reaction was carried out over a 24 h period and during this time the viscosity of the polymer solution increased. PAA was synthesized in triplicate for reproducibility and was immediately used for grafting. Any unused PAA solution was stored at 4 °C.

2.2.3. Preparation of PAA graft/cross-linked PVA hydrogel samples using DCC/DMAP

PVA discs (seven samples) were removed from distilled water and placed in a 100 ml vessel containing 60 ml of NMP or 60 ml of DMF, mixed and heated to 37 °C for 72 h. Over the 72 h fresh solvent was exchanged every 20 h for a total of three exchanges. Immediately following completion of the solvent exchange steps PAA (5 mmol), DCC (5.5 mmol), PVA discs and DMAP (5 mmol) in NMP or DMF (30 ml) were mixed at 150 rpm and held at 37 °C for 48 h. A nitrogen blanket was maintained throughout the experiment. Upon completion of the reaction the PVA discs were removed from the reaction vessel and washed several times with water (60 ml) and then with PBS (60 ml) over a Buchner funnel. Grafted/cross-linked samples were then placed in PBS and stored at room temperature for 72 h prior to cell culture experiments and mechanical testing.

2.3. Characterization

2.3.1. Fourier transform infrared (FTIR) spectroscopy

The attenuated total reflectance-Fourier transform infrared (ATR-FTIR) (Pike Technologies Inc., Madison, WI) spectra were recorded using a Bruker Vector 22 FTIR spectrometer (Milton, ON) and obtained with a horizontal ATR attachment using a diamond crystal. Spectra were recorded with 128 averaged scans at 4 cm^{-1} resolution, displayed in absorption mode and ratioed to the appropriate background spectra. All spectra were normalized and smoothed using OPUS-NT 3.1 software to enhance the signal-to-noise ratio.

2.3.2. Proton (^1H) and carbon (^{13}C) nuclear magnetic resonance (NMR) spectroscopy

Solid-state magic angle spinning (MAS) ^1H NMR and ^{13}C NMR spectra were recorded on a Varian Infinity Plus 400 spectrometer equipped with a Varian 3.2 mm (spinning rate 10.0 kHz) and/or a Varian 4.0 mm (spinning rate 12 kHz) HXY probe. ^1H and ^{13}C NMR spectra were referenced with respect to TMS ($\delta(^1H) = 0.0$ ppm and $\delta(^{13}C) = 0.0$ ppm) by setting the ^1H peak of adamantane to 1.48 ppm and the high frequency ^{13}C peak of adamantane to 38.56 ppm [22]. Additionally, free induction decays (FIDs) were processed with 50 Hz line broadening for the ^{13}C (single pulse) experiments. ^1H NMR spectra were acquired using a Bloch decay (single pulse) experiment with a relaxation delay of 10 s, spectral width between 100 and 200 kHz, pulse width between 3 and 3.5 μs and acquisition time between 10 and 250 ms with between

16 and 24 transients. ^{13}C NMR spectra were acquired in a similar manner using either a single pulse or variable-amplitude cross-polarization experiment with ^{1}H TPPM decoupling applied during acquisition [23]. For the ^{13}C single pulse experiments a relaxation delay of 30 s, spectral width of 50 kHz, pulse width of 1.5 μs acquisition time between 40 and 100 ms with between 400 and 6000 transients was used. The ^{13}C variable-amplitude cross-polarization spectra were acquired with a relaxation delay of 10 s, spectral width between 50 and 100 kHz, acquisition time between 10 and 20 ms and contact time of 0.25 ms with between 72 and 270 transients. ACD Labs Version 11.0 software was used to process the ^{13}C NMR data.

2.3.3. X-ray photoelectron spectroscopy (XPS)

XPS experiments were performed using a Kratos Axis Ultra spectrometer using an integrated magnetic immersion lens and charge neutralization system with a spherical mirror analyzer. The instrument consisted of a micro-channel plate and phosphor detection system to provide parallel imaging with high spatial resolution and high sensitivity. Measurements were acquired using a 210 W Al Kα monochromatic X-ray source and samples were tested in hybrid mode with 90° take-off angles. The pass energy of the survey scan was 160 eV and of the high resolution scan was 20 eV. Multi-peak fitting and data analysis were performed using CasaXPS software.

2.3.4. Mechanical testing

Tensile tests were performed on PVA and PAA-g/c-PVA hydrogels. Tensile experiments on all samples were carried out using an INSTRON 8872 servo-hydraulic material testing system equipped with a 1 kg load cell at a cross-head speed of 40 mm s^{-1} to a maximum of 60% strain. The samples were immersed in PBS in a Plexiglas tank at 37 °C for 1 h prior to tensile testing. Sample preconditioning (10 loading and unloading cycles) was completed prior to tensile testing as previously described [14]. Load versus displacement data were recorded and converted into engineering stress–engineering strain using the sample thickness and initial gauge length after preconditioning. All samples were secured using custom tissue grips with an ~10 mm grip to grip distance.

2.3.5. Scanning electron microscopy (SEM)

For SEM the PVA and PAA-g/c-PVA samples were removed from the sample storage solution (PBS or water) and immersed in 100% ethanol overnight followed by drying using a critical point dryer (Samdri PVT-3B Critical Point Dryer, Tousimis Research Corp., Rockville, MD). The dried samples were then immersed in liquid nitrogen and fractured so cross-sectional areas of the hydrogels could be examined. Electron micrographs were taken in a Leo (Zeiss) 1530 field emission scanning electron microscope. An accelerating voltage of 1 keV was selected to minimize charging and possible damage to the porous structure.

2.4. Cell culture

Primary cultures of porcine descending aorta ECs were isolated as previously described [24]. ECs were maintained in endothelial growth medium (EGM) with 5% fetal bovine serum, 1% penicillin/streptomycin and a bullet kit containing rhEGF, rhFGF-B, VEGF, R^3-IGF-1, gentamicin/amphotericin, hydrocortisone, and ascorbic acid (Lonza Canada, Shawinigan, QC). ECs (passages 3–5) were independently seeded onto PVA hydrogels and PAA-g/c-PVA hydrogels at an initial cell density of 25,000 cells cm^{-2}. Coverslips were seeded at the same density to serve as time-matched controls. Cell growth and cell adhesion were examined at 4, 24 and 48 h.

2.4.1. Immunolabeling and confocal microscopy

ECs seeded on hydrogels and coverslips were stained with polyclonal rabbit anti-human Von Willebrand factor primary IgG (A0082, 1:50) (Dako Canada, Mississauga, ON) and AlexaFluor® 488 goat anti-rabbit IgG secondary antibody (1:200) (Invitrogen Molecular Probes, Eugene, OR). Nuclei were labeled with Hoechst 33,342. Immunolabeled coverslips and hydrogels were imaged with a Zeiss LSM 410 laser scanning confocal microscope system and LSM-PC imaging software (Carl Zeiss Canada, Toronto, ON).

2.5. Statistical analysis

Data analysis was carried out using OriginPro Version 8.0 (OriginLab Software, Northampton, MA) statistical software package. Data were analyzed by either a one-way analysis of variance (ANOVA) or Student's *t*-test.

3. Results and discussion

For soft tissue replacements, such as small diameter vascular grafts, the material of choice has to satisfy several property requirements. These include biocompatibility, matching of mechanical properties and hemocompatibility. Using physically cross-linked PVA prepared by a low temperature thermal cycling process, the first two property requirements can be met. However, hemocompatibility remains a challenge. In addition to the traditional approach of coating PVA with bioactive agents, such as heparin, growth factors, and other anticoagulant peptide sequences [18], another alternative is to create a "living" surface by immobilizing ECs onto the PVA surface. There have been several reports on creating a cell-friendly PVA surface using this approach [3–5,12,25]. We have previously demonstrated that physically cross-linked PVA hydrogels can be functionalized with a cell adhesion protein, fibronectin, using a simplified reaction without the CDI activation step that is necessary for chemically (glutaraldehyde) cross-linked PVA hydrogels. The functionalized surface became cell compatible and showed good endothelization. In our search for a novel cell-compatible material we synthesized ethylene diamine tetraacetic dianhydride derived PAA and demonstrated its compatibility with vascular cells [19]. To take advantage of this favorable cell compatibility of PAA for physically cross-linked PVA we investigated the grafting/cross-linking of PAA onto the PVA hydrogel surface via an esterification reaction using DCC as activating agent and DMAP as catalyst.

DCC is a well-known and widely used activating/dehydrating agent for the synthesis of various organic compounds, including amides, proteins and esters [26]. We were interested in using DCC to promote esterification between a secondary alcohol in PVA and a carboxylic acid in PAA. The esterification of alcohols is possible using DCC without the aid of a catalyst, but requires an acidic or basic medium and heat [27–29] and often results in low product yields, and in our case potentially minimized the level of grafting achievable. Several studies have reported excellent polymer yields when synthesizing esters by using DCC as the activating agent in combination with DMAP as a catalyst [30,31]. The DCC/DMAP system was adopted in our esterification reaction between PVA and PAA.

3.1. Polymer synthesis: PAA-g/c-PVA

PAA-g/c-PVA hydrogels were synthesized using equimolar amounts of PAA, PVA and DMAP and an excess of DCC. This excess was necessary to maximize the yield of the esterification reaction. Fig. 1 depicts the esterification reaction between PAA and PVA in the presence of DCC and DMAP. The mechanism involves DCC/

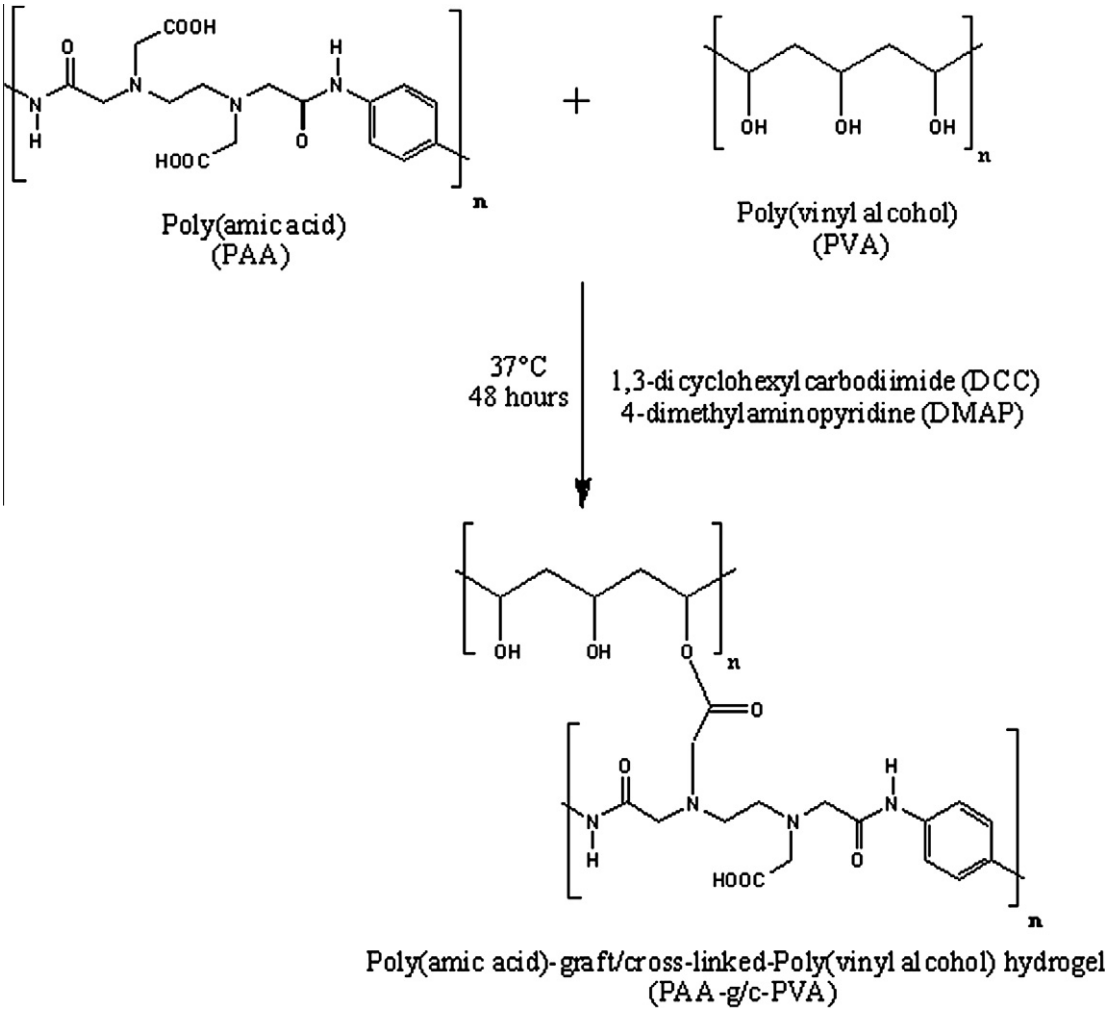

Fig. 1. Synthesis of PAA-g/c-PVA hydrogel.

DMAP selectively activating the carboxyl group in the PAA to form an intermediate complex. The intermediate complex reacts with the hydroxyl groups on the PVA surface to produce an ester linkage with dicylcohexylurea (DCU) as the by-product [32]. The reaction allows at least one of the carboxylic acids in PAA to react with an alcohol group in PVA. As a result, both inter- and intramolecular cross-linking can occur. The by-product DCU was not soluble in the solvent used (NMP or DMF) and was removed by filtration and successive water and PBS washings at the end of the reaction. The PAA-g/c-PVA hydrogel formed by the esterification reaction resulted in a rubbery, semi-opaque, flexible hydrogel. All grafted samples were characterized using FTIR, solid-state ^{1}H NMR and ^{13}C NMR, XPS, SEM, mechanical testing and then fixed on glass coverslips and tested for EC attachment in vitro.

3.2. Structural characterization

3.2.1. FTIR

To determine the success of the esterification reaction ATR-FTIR spectra before and after the grafting reaction were obtained. Fig. 2 illustrates the FTIR spectra of PAA-g/c-PVA, PVA and PAA. The main vibration bands present in the grafted polymer were at 3386, 2937, 2903, 1652, 1507, 1410, 1309, 1261 and 1100 cm^{-1}. The broad absorption between 3650 and 3050 cm^{-1} refers to the OH stretching region [33]. In particular, the OH peak represents the carboxylic acid groups on the PAA polymer and the alcohol groups on the PVA

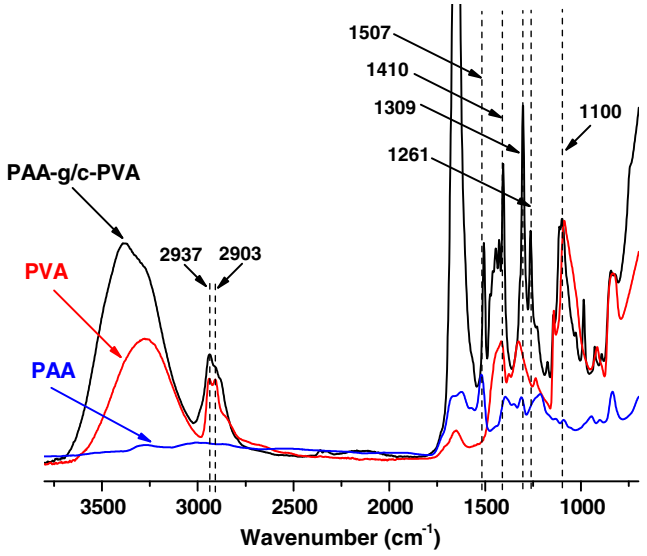

Fig. 2. Representative ATR-FTIR spectra for PAA-g/c-PVA hydrogel, PVA hydrogel and PAA.

polymer. Sharp peaks at 2937 and 2903 cm^{-1} (between 3000 and 2800 cm^{-1}) represent the CH absorption bands in the aliphatic region in the PVA and PAA polymers, as well as the aromatic region

in the PAA polymer, which includes CH and CH_2 stretching and bending vibrations. The sharp and large peaks between 1748 and 1546 cm^{-1} represent a series of C=O stretching bands [34] indicative of an ester (1750–1730 cm^{-1}), a carboxylic acid (1720–1700 cm^{-1}) and an amide I peak (1675 cm^{-1}). Due to the broadness of the peak, it is difficult to distinguish each carbonyl peak. The peak at 1507 cm^{-1} corresponds to the amide II peak present in the backbone of the PAA polymer, which corresponds to the combination band of the N–H bending and C–N stretching vibrations. The medium peak at 1410 cm^{-1} coincides with the CH_2 and CH_3 bending vibrations in the backbone of the grafted polymer. The additional strong peaks at 1309 and 1261 cm^{-1} correspond to a C–O stretch and provide evidence that an ester and an acid were present. The peak at approximately 1100 cm^{-1} also represents a C–O stretch and is indicative of the crystallinity of PVA [35]. The intensities of the functional groups present in the grafted polymer appeared sharp in the infrared region, however, many of the peaks observed overlapped, making it difficult to pinpoint functionality.

3.2.2. Solid-state ^1H NMR and ^{13}C NMR

To directly observe chemical species and verify molecular structures existing in the grafted products high resolution solid-state ^1H NMR and ^{13}C NMR spectra were obtained for PVA and PAA-g/c-PVA, shown in Figs. 3 and 4. Fig. 3A and B displays the solid-state ^1H NMR and ^{13}C NMR spectra of PVA, respectively. The NMR confirmed the chemical composition of the repeating chain in PVA and gave an insight into its tacticity. The ^1H MAS-NMR spectra of the cycle 6 PVA hydrogel sample consisted of two resolved resonances at 2.05 and 3.76 ppm, which correspond to $–CH_2–$ (a) and –CH– (b), respectively. The peak at 7.18 ppm was most probably due to moisture in the environment and the result of a wide distribution of hydrogen bonding [36]. The corresponding ^{13}C MAS-NMR spectra of cycle 6 PVA hydrogel samples clearly displays the methylene carbon ($–CH_2–$) peak at 45.60 ppm and methine carbon (–CH–) resonances at 65.05, 70.88 and 77.20 ppm. The methine peaks at 70.88 and 77.20 ppm correspond to an isotactic triad with two intramolecular hydrogen bonds and the remaining methine peak at 65.05 ppm corresponds to a syndiotactic triad with no intervening intramolecular hydrogen bonds [37].

Fig. 4 displays the solid-state variable-amplitude cross-polarization ^{13}C NMR spectra of PAA-g/c-PVA synthesized in NMP. There were 12 noticeable peaks which appeared at approximately δ 173.79, δ 164.54, δ 152.86, δ 131.94, δ 120.75 and δ 76.97, δ 71.13, δ 65.29, δ 45.34, δ 30.75, δ 26.37, δ 22.96 ppm. The three downfield signals at δ 173.79 (labeled j), δ 164.54 (labeled l and c) and δ 152.86 ppm (labeled a) represent the acid, ester and the amide carbonyl carbon which are all commonly observed at higher frequencies [34]. The grafted spectrum also showed two broad sig-

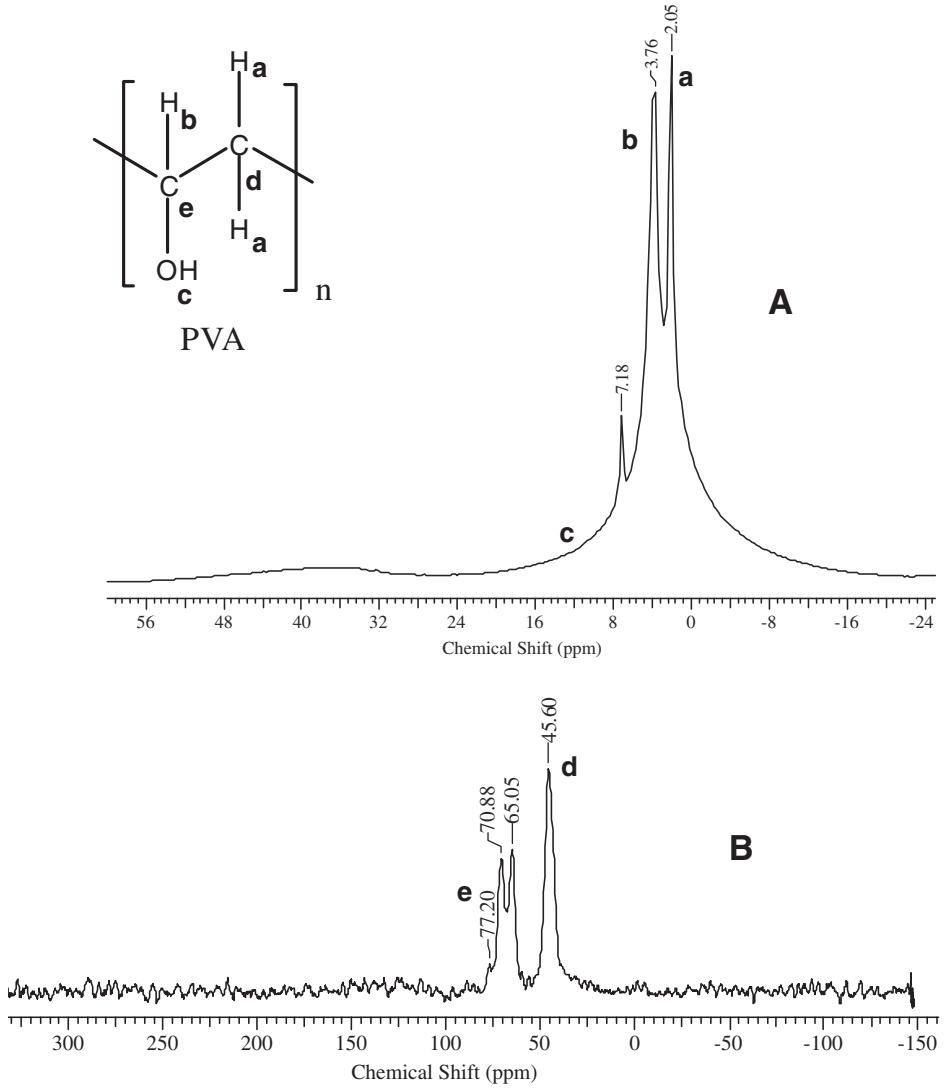

Fig. 3. Solid-state (A) ^1H NMR spectrum and (B) ^{13}C NMR spectrum of PVA hydrogel.

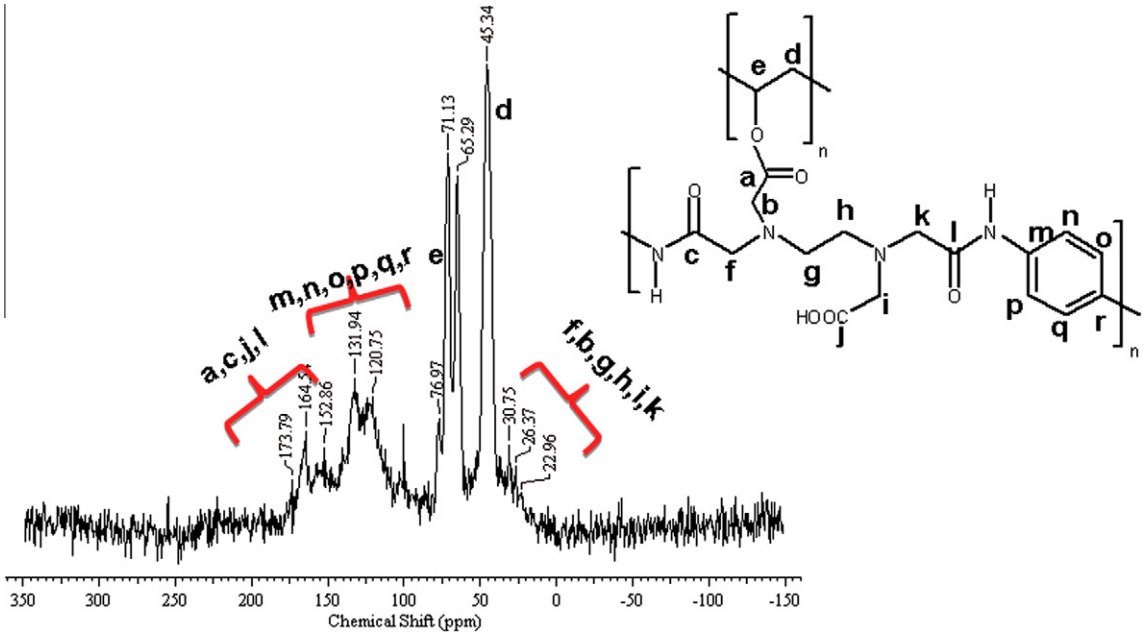

Fig. 4. Solid-state variable-amplitude cross-polarization ^{13}C NMR spectrum of PAA-g/c-PVA.

nals at approximately δ 131.94 and δ 120.75 ppm, representing the aromatic carbons in the backbone of the PAA polymer [19]. The next four signals at δ 76.97, δ 71.13, δ 65.29, δ 45.34 ppm represent the methine (labeled e) and methylene (labeled d) carbons in the backbone of the PVA polymer previously analyzed in Fig. 3B. Fig. 4 shows the methine peak at a lower frequency in the grafted polymer. This subtle shift is indicative of attachment. Beyond the methylene peak associated with PVA, there were a series of overlapping peaks which represent the saturated carbon atoms in the backbone of the grafted polymer. These peaks are a series of R–CH_2- (labeled f, b, g, h, i and k) groups. The presence of a carbonyl carbon affiliated with an ester and the absence of peaks associated with the by-product (DCU) indicate conclusively that an ester was formed during the grafting process and that the material was free from contamination.

3.2.3. XPS

XPS was used to verify the bonding environment and elemental distribution on the grafted polymer surface. Fig. 5 illustrates the survey scans of PVA, PAA and PAA-g/c-PVA hydrogels with their respective core level spectra. The high resolution C_{1s} spectrum of the PVA hydrogel (Fig. 5B) was fitted with four peak components using CasaXPS (Casa Software Ltd.) based on the built-in Marquardt–Levenberg optimization algorithm [38] with binding energies (BEs) at 285.0 eV for the C–H and C–C species, at 286.5 eV for the C–O species, at 288.1 eV for the C=O species and at 289.4 eV for the O=C–O species. The O_{1s} core level spectrum (Fig. 5C) was curve fitted with one peak component, with a BE at 532.7 eV for the C–O species. Similarly, the high resolution C_{1s} spectrum of PAA (Fig. 5E) was fitted with five peak components, with BEs at 284.9 eV for the C–H and C–C species, at 285.7 eV for the C–N species, at 286.3 eV for the aromatic C species, at 287.9 eV for the O=C–N species and at 288.9 eV for the O=C–O species. The O_{1s} core level spectrum (Fig. 5F) was curve fitted with three peak components, with BEs at 531.0 eV for O=C–N species, at 532.0 eV for the O^*–C=O species and at 533.3 eV for the O–C=O^* species. The N_{1s} core level spectrum (Fig. 5G) was curve fitted with three peak components, with BEs at 399.8 eV for the N–C species, at 400.7 eV for the N–C=O species and at 401.8 eV for the N–H species [39]. Lastly, the high resolution C_{1s} spectrum of the PAA-g/c-PVA hydrogel (Fig. 5I) was fitted with five peak components, with BEs at 285.0 eV for the C–H and C–C species, at 285.8 eV for the C–O and C–N species, at 286.6 eV for the C–OH and aromatic C species, at 288.0 eV for the O=C–N species and at 289.1 eV for the O=C–O species. The O_{1s} core level spectrum (Fig. 5J) was curve fitted with three peak components, with BEs at 531.3 eV for O=C–N species, at 532.5 eV for the C–O species and at 533.8 eV for the O–C=O^* species. The N_{1s} core level spectrum (Fig. 5K) was curve fitted with two peak components, with BEs at 399.8 eV for the N–C species and 400.7 eV for the N–C=O species [39]. PVA and PAA-g/c-PVA clearly showed a different distribution of oxygen and carbon atoms, in addition to the appearance of nitrogen atoms in the grafting material. There was a subtle shift of carbon peaks to a lower frequency from PVA to PAA-g/c-PVA. The most noticeable difference was the absence of carboxylic acid groups (O^*–C=O) from PAA to the PAA-g/c-PVA material. The peak corresponding to –COOH was not detected, further indicating that the majority of alcohol groups on the PVA surface had reacted. Given the detection sensitivity of XPS (0.3–0.4 at.%), we can estimate the degree of grafting on the PVA surface to be >50%. The O–C=O and O=C–N peaks implied the formation of an ester bond and the presence of an amide bond in the grafted material. Additionally, the presence of the N–C and N–H peaks observed in the N_{1s} core level spectrum for the PAA-g/c-PVA material indicated that PAA was successfully grafted onto PVA. The survey scans showed trace amounts of other elements, as indicated in Table 1. The other elements were due to the residual salt from the PBS buffer left on the surface of the samples.

3.2.4. SEM

The morphology of the PVA and PAA-g/c-PVA hydrogels were observed using SEM. Fig. 6A and B shows cross-sections of the PVA hydrogel before and after grafting (PAA-g/c-PVA). These samples were dried using critical point drying methods in order to preserve their cross-sectional morphologies. A decrease in pore size of PVA after grafting was apparent. Using Image J (National Institutes of Health) the average pore diameters in PVA and PAA-g/c-PVA were determined as 320 ± 70 and 210 ± 50 nm, respectively. This decrease in pore size was most likely a result of the use of the

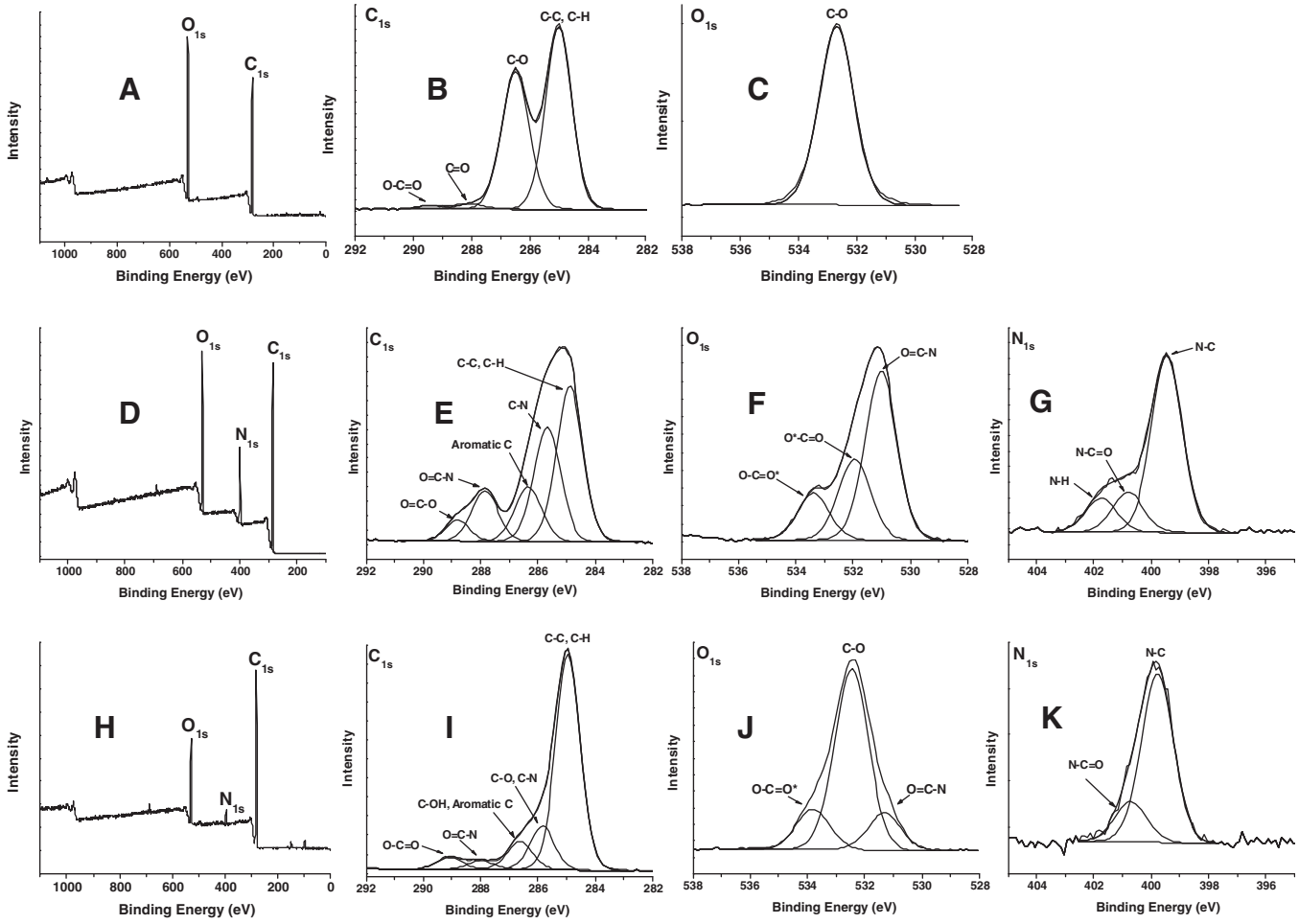

Fig. 5. X-ray photoelectron spectroscopy survey scan of (A) PVA and core level spectra of (B) carbon and (C) oxygen, (D) PAA and core level spectra of (E) carbon, (F) oxygen and (G) nitrogen and (H) PAA-g/c-PVA and core level spectra of (I) carbon, (J) oxygen and (K) nitrogen.

Table 1
Elemental distribution of PVA and PAA-g/c-PVA.

Element	PVA (at.%)	PAA-g/c-PVA (at.%)
Carbon	73.6	78.3
Oxygen	24.3	14.1
Nitrogen	–	5.6
Trace elements (sodium, phosphorus, and silicon)	2.1	2.0
Total	100	100

dehydrating reagent (DCC) in the grafting reaction which led to partial pore collapse [40].

3.2.5. Mechanical testing

The tensile mechanical properties of the PVA hydrogel before grafting and the product PAA-g/c-PVA are shown in Fig. 7. The stress–strain curve for PAA-g/c-PVA was above that of the PVA hydrogel, indicating that there was an overall increase in the stiffness of the PAA-g/c-PVA material relative to that of the PVA hydrogel. The elastic moduli of PVA and PAA-g/c-PVA at a strain of 0.6

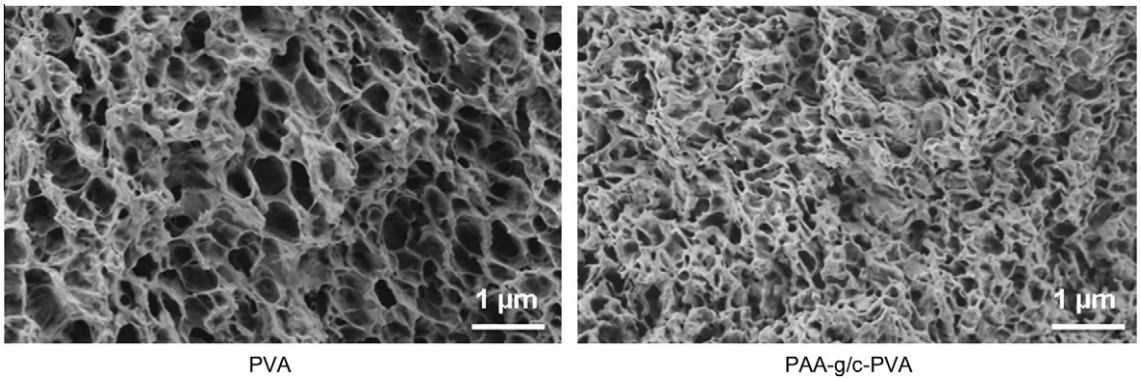

Fig. 6. Scanning electron micrographs of cross-sections of (A) PVA and (B) PAA-g/c-PVA synthesized in NMP.

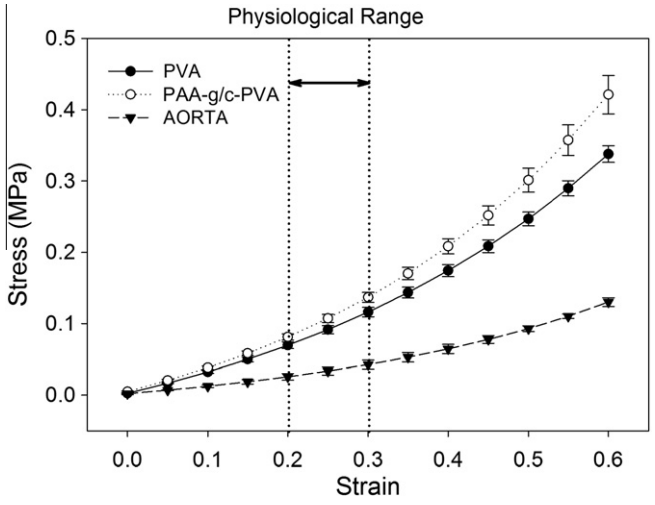

Fig. 7. Stress–strain response of poly(vinyl alcohol) (PVA) and poly(amic acid) graft/cross-linked poly(vinyl alcohol) hydrogel (PAA-g/c-PVA) synthesized in NMP.

were 1.02 ± 0.06 and 1.36 ± 0.13 MPa, respectively. This represents an increase of about 30%. This increase is significantly smaller than that observed for a comparable functionalization reaction on the PVA hydrogel using fibronectin in which a drying step was involved. Since our grafting reaction does not involve a drying step, the pore size reduction of the PAA-g/c-PVA shown in Fig. 6B due to partial pore collapse would be expected to be less than that of the fibronectin functionalization reaction, as observed. The 30% increase in elastic modulus at a strain of 0.6 may seem to be quite large, however, since the normal physiological strain range of aortic tissue is in the range 0.2–0.3 [14,41] the difference is quite small. The moduli within this strain range for PVA and PAA-g/c-PVA were 0.46 ± 0.02 and 0.55 ± 0.03 MPa, respectively. This represents an increase of only about 19%, which is quite small. The use of a dehydrating agent (DCC), which has been shown to decrease pore size, as seen in Fig. 6B, is mostly likely the reason why there was a small stiffening effect. With respect to the esterification reaction, this small stiffening effect further showed that although intramolecular cross-linking was a possible reaction, it was unlikely to be the dominant reaction. This represents the best results so far in preserving the structure and mechanical properties of the functionalized PVA hydrogel.

3.3. Cell culture

ECs were seeded onto glass coverslips, PVA hydrogel discs and PVA-g–PAA hydrogel discs with a cell density of 25,000 cells cm^{-2} for all trials. The cells were uniformly seeded onto the grafted gels and were cultured for up to 48 h. Direct contact of ECs with the grafted hydrogels not only exposed them to the material but also to trace amounts of unreacted monomer, catalyst and cross-linking agents that may have also been present on the culture plate. Fig. 8A and B displays confocal images of ECs (nuclei appear blue, while Von Willebrand factor, a cytoplasmic protein, is labeled green) in contact with the glass coverslips, PVA and PVA-g/c-PAA hydrogels at 4, 24 and 48 h. It can be seen that the ECs spread out well and adhered to both the coverslips and grafted hydrogels over 48 h. A confluent layer was formed by the ECs shortly after this time point on both surfaces. As anticipated no cells adhered to the PVA hydrogels. ECs seeded on PAA-g/c-PVA displayed adhesion at 4 h, indi-

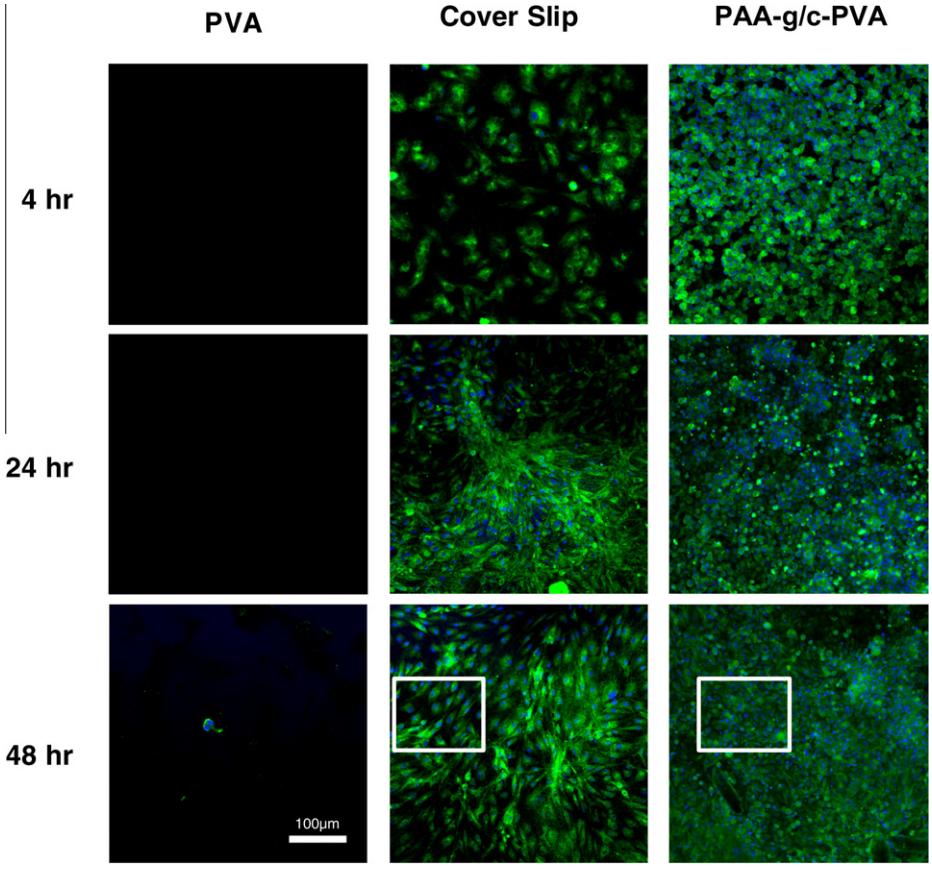

Fig. 8. (A) Confocal images of endothelial cells at 4, 24 and 48 h on PVA hydrogel, on an uncoated (control) coverslip and on PAA-g/c-PVA. (B) Confocal images of endothelial cells at 48 h on glass coverslips and on PAA-g/c-PVA focusing on the boxed areas in (A).

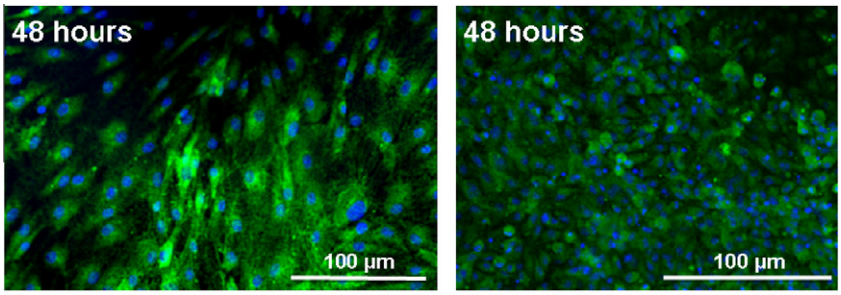

Fig. 8 (*continued*)

cating that PAA-g/c-PVA was an adequate adhesion surface. The ECs adherent on glass coverslips displayed a normal cell morphology and cell growth pattern, whereas ECs in contact with PVA over the same duration failed to show any cell adhesion and spreading. With regard to the grafted material, cell morphology and cell density differed from those on the glass coverslips in the first 4 h, but morphology and growth pattern seemed similar to those of the controls at 48 h (Fig. 8B). Furthermore, ECs in contact with the grafted hydrogel, as seen in Fig. 8B (expanded area outlined in Fig. 8A), did not appear rounded and clumped, indicative of poor cell adhesion and health, as these cells are normally adherent. Clearly, the ECs had adapted to grow on the PAA-g/c-PVA hydrogel surface within a short timeframe. This visual appearance of ECs on the grafted hydrogel was consistent with our previous work, in which we demonstrated that PAA is not cytotoxic to cells in a quantitative tetrzolium-based colorimetric WST-1 assay [19].

4. Conclusion

In this work we have demonstrated the use of an esterification reaction to graft the cell-compatible ethylene diamine tetraacetic acid dianhydride derived PAA onto a mechanically tuned physically cross-linked PVA hydrogel prepared via a low temperature thermal cycling process. Cell compatibility using primary porcine vascular ECs has also been demonstrated. Moreover, the grafting reaction was carried out without the necessity of dehydrating the PVA hydrogels, thus allowing the PAA-g/c-PVA material to retain most of the tensile properties of the original PVA hydrogel. This approach to cell compatibility can be contrasted with most of the approaches reported in the literature, where PVA hydrogels were chemically cross-linked using multiple reaction steps. The ability to conserve most of the mechanical properties of the PVA hydrogel in PAA-g/c-PVA is important for the creation of a cell-compatible interface for PVA–tissue hybrid development. Our approach would be especially useful for cardiovascular devices, such as small diameter vascular grafts, where both hemocompatibility and mechanical properties matching are important requirements.

Acknowledgements

This work was supported by scholarships from the Canadian Institutes of Health Research (CIHR), Heart and Stroke Foundation of Ontario, Ontario Graduate Scholarship funds, Ontario Graduate Scholarship in Science and Technology funds and by the Western Graduate Research Scholarship. We would also like to thank the Canadian Institutes of Health for a Research Training Grant in Vascular Research (D.P. and A.H. were both CIHR Training Fellows). In addition to the scholarship funds, the authors thank Dr Mathew Willans, Dr Kenneth Wong and Mark Biesinger for their technical assistance with solid-state NMR, SEM and XPS, respectively. The authors would also like to thank Darius Strike for EC isolation and Dr Kem Rogers for the use of his cell culture facilities.

Appendix A. Figures with essential colour discrimination

Certain figures in this article, particularly Figures 2, 4 and 8 are difficult to interpret in black and white. The full colour images can be found in the on-line version, at doi:10.1016/j.actbio.2010.07.038.

References

[1] Ratner BD, Shen TTs. Device and method for intraocular drug delivery. Seattle, WA, USA: University of Washington; 2008.
[2] Feingold-Leitman D, Zussman E, Seliktar D. In vitro evaluation of a composite scaffold made from electrospun nanofibers and a hydrogel for tissue engineering. J Bionanosci 2009;3:45–57.
[3] Sailaja GS, Sreenivasan K, Yokogawa Y, Kumary TV, Varma HK. Bioinspired mineralization and cell adhesion on surface functionalized poly(vinyl alcohol) films. Acta Biomater 2009;5(5):1647–55.
[4] Zajaczkowski MB, Cukierman E, Galbraith CG, Yamada KM. Cell–matrix adhesions on poly(vinyl alcohol) hydrogels. Tissue Eng 2003;9(3):525.
[5] Sugawara T, Matsuda T. Photochemical surface derivatization of a peptide containing Arg–Gly–Asp (RGD). J Biomed Mater Res 1995;29(9):1047–52.
[6] Shi R, Zhu A, Chen D, Jiang X, Xu X, Zhang L, et al. Degradation of starch/PVA films and biocompatibility evaluation. J Appl Polym Sci 2010;115(1):346–57.
[7] Mansur HS, de Souza Costa-Júnior E, Mansur AAP, Barbosa-Stancioli EF. Cytocompatibility evaluation in cell-culture systems of chemically crosslinked chitosan/PVA hydrogels. Mater Sci Eng C 2009;29(5):1574–83.
[8] de Souza Costa-Júnior E, Pereira M, Mansur H. Properties and biocompatibility of chitosan films modified by blending with PVA and chemically crosslinked. J Mater Sci Mater Med 2009;20(2):553–61.
[9] Mathews DT, Birney YA, Cahill PA, McGuinness GB. Vascular cell viability on polyvinyl alcohol hydrogels modified with water-soluble and -insoluble chitosan. J Biomed Mater Res Part B Appl Biomater 2008;84B(2):531–40.
[10] Liu Y, Vrana NE, Cahill PA, McGuinness GB. Physically crosslinked composite hydrogels of PVA with natural macromolecules: structure, mechanical properties, and endothelial cell compatibility. J Biomed Mater Res Appl Biomater 2009;90B(2):492–502.
[11] Shalumon KT, Binulal NS, Selvamurugan N, Nair SV, Menon D, Furuike T, et al. Electrospinning of carboxymethyl chitin/poly(vinyl alcohol) nanofibrous scaffolds for tissue engineering applications. Carbohydr Polym 2009;77(4):863–9.
[12] Jiang T et al. Heparinized poly(vinyl alcohol)–small intestinal submucosa composite membrane for coronary covered stents. Biomed Mater 2009;4(2):025012.
[13] Hayami T, Matsumura K, Kusunoki M, Nishikawa H, Hontsu S. Imparting cell adhesion to poly(vinyl alcohol) hydrogel by coating with hydroxyapatite thin film. Mater Lett 2007;61(13):2667–70.
[14] Millon LE, Mohammadi H, Wan WK. Anisotropic polyvinyl alcohol hydrogel for cardiovascular applications. J Biomed Mater Res Appl Biomater 2006;79B(2):305–11.
[15] Williams C, Kitlas P, Nickel T, Mejia L. BioDynamic test instrument for characterization of tissues and biomaterials. Paper presented at AIChE annual meeting. San Fransisco, CA; 2006.
[16] Kannan RY, Salacinski HJ, Butler PE, Hamilton G, Seifalian AM. Current status of prosthetic bypass grafts: a review. J Biomed Mater Res Appl Biomater 2005;74B(1):570–81.
[17] Xue L, Greisler HP. Biomaterials in the development and future of vascular grafts. J Vasc Surg 2003;37(2):472–80.
[18] Thomas AC, Campbell GR, Campbell JH. Advances in vascular tissue engineering. Cardiovasc Pathol 2003;12(5):271–6.
[19] Padavan D, Hamilton A, Boughner D, Wan WK. Synthesis and in vitro biocompatibility assessment of a poly(amic acid) derived from

ethylenediaminetetraacetic dianhydride. J Biomater Sci Polymer Ed, accepted for publication. doi:10.1163/092050610X490149.
[20] Wan WK, Campbell G, Zhang ZF, Hui AJ, Boughner DR. Optimizing the tensile properties of polyvinyl alcohol hydrogel for the construction of a bioprosthetic heart valve stent. J Biomed Mater Res 2002;63(6):854–61.
[21] Millon LE, Nieh MP, Hutter JH, Wan WK. SANS characterization of an anisotropic poly(vinyl alcohol) hydrogel with vascular applications. Macromolecules 2007;40:3655–62.
[22] Hayashi S, Hayamizu K. Chemical-shift standards in high-resolution solid-state NMR (1) C-13, Si-29 and H-1 nuclei. Bull Chem Soc Jpn 1991;64(2):685–7.
[23] Bennett AE, Rienstra CM, Auger M, Lakshmi KV, Griffin RG. Heteronuclear decoupling in rotating solids. J Chem Phys 1995;103(16):6951–8.
[24] Rogers KA, Boden P, Kalnins VI, Gotlieb AI. The distribution of centrosomes in endothelial cells of non-wounded and wounded aortic organ cultures. Cell Tissue Res 1986;243(2):223.
[25] Nuttelman CR, Mortisen DJ, Henry SM, Anseth KS. Attachment of fibronectin to poly(vinyl alcohol) hydrogels promotes NIH 3T3 cell adhesion, proliferation, and migration. J Biomed Mater Res 2001;57(2):217.
[26] Holmberg K, Hansen B. Ester synthesis with dicyclohexylcarbodiimide improved by acid catalysts. Acta Chem Scand 1979;B33:410.
[27] Shelkov R, Nahmany M, Melman A. Selective esterifications of alcohols and phenols through carbodiimide couplings. Org Biomol Chem 2004;2(3):397.
[28] Zengin G, Huffman JW. Naphthyl ester synthesis using 1,3-dicyclohexylcarbodiimide. Synthesis 2004;2004(12):1932–4.
[29] Klesper E, Strasilla D, Berg MC. ^{1}H-NMR of the esterification of syndiotactic poly(methacrylic acid) with carbodiimides – II. Esterification with benzylalcohol and trifluoroethanol. Eur Polym J 1979;15(6):593–601.
[30] Rauf A, Parveen H. Direct esterification of fatty acids with phenylalkanols by using dicyclohexylcarbodiimide. Eur J Lipid Sci Technol 2004;106(2):97–100.
[31] Trull FR, Lightner DA. Synthesis of dipyrrinone esters using carbodiimide reagents. Tetrahedron 1991;47(10–11):1945–56.
[32] Stryer L. Biochemistry. 3rd ed. New York: W.H. Freeman and Co.; 1988.
[33] Pavia DL, Lampman GM, Kriz GS. Introduction to spectroscopy: a guide for students of organic chemistry. 3rd ed. Fort Worth, TX: Harcourt College Publishers; 2001.
[34] Pavia DL. Introduction to spectroscopy. 4th ed. Belmont, CA: Brooks/Cole, Cengage Learning; 2009.
[35] Peppas NA. Infrared spectroscopy of semicrystalline poly(vinyl alcohol) networks. Makromol Chem 1977;178(2):595–601.
[36] Horii F, Hu SH, Deguchi K, Sugisawa H, Ohgi H, Sato T. H-1 CRAMPS spectra of poly(vinyl alcohol) films with different tacticities. Macromolecules 1996;29(9):3330–1.
[37] Lai S, Casu M, Saba G, Lai A, Husu I, Masci G, et al. Solid-state ^{13}C NMR study of poly(vinyl alcohol) gels. Solid State Nucl Magn Reson 2002;21(3/4):187–96.
[38] Press WH. Numerical recipes in C: the art of scientific computing. 2nd ed. Cambridge, UK: Cambridge University Press; 1992.
[39] Beamson G, Briggs D. High resolution XPS of organic polymers. New York: John Wiley and Sons; 1992.
[40] Patachia S, Valente AJM, Baciu C. Effect of non-associated electrolyte solutions on the behaviour of poly(vinyl alcohol)-based hydrogels. Eur Polym J 2007;43(2):460–7.
[41] Hansen B, Menkis AH, Vesely I. Longitudinal and radial distensibility of the porcine aortic root. Ann Thorac Surg 1995;60(2):S384–90.